PCP
PLANT & CELL PHYSIOLOGY

Sugar Uptake in the Aril of Litchi Fruit Depends on the Apoplasmic Post-Phloem Transport and the Activity of Proton Pumps and the Putative Transporter *LcSUT4*

Teng-Duan Wang[1,2], Hui-Fen Zhang[1,2], Zi-Chen Wu[1], Jian-Guo Li[1], Xu-Ming Huang[1,*] and Hui-Cong Wang[1,*]

[1]Physiological Laboratory for South China Fruits, College of Horticulture, South China Agricultural University, Guangzhou, 510642, PR China
[2]These authors contributed equally to this work.
*Corresponding authors: Hui-Cong Wang, E-mail, wanghc1972@263.net; Fax, +86-20-85280228;
Xu-Ming Huang, E-mail, huangxm@scau.edu.cn; Fax, +86-20-85280228.
(Received October 4, 2014; Accepted November 18, 2014)

The post-phloem unloading pathway and the mechanism of sugar accumulation remain unclear in litchi fruit. A combination of electron microscopy, transport of phloem-mobile symplasmic tracer (carboxyfluorescein, CF) and biochemical and molecular assays was used to explore the post-phloem transport pathway and the mechanism of aril sugar accumulation in litchi. In the funicle, where the aril originates, abundant plasmodesmata were observed, and CF introduced from the peduncle diffused to the parenchyma cells. In addition, abundant starch and pentasaccharide were detected and the sugar concentration was positively correlated with activities of sucrose hydrolysis enzymes. These results clearly showed that the phloem unloading and post-phloem transport in the funicle were symplastic. On the other hand, imaging of CF showed that it remained confined to the parenchyma cells in funicle tissues connecting the aril. Infiltration of both an ATPase inhibitor [eosin B (EB)] and a sucrose transporter inhibitor [*p*-chloromercuribenzene sulfonate (PCMBS)] inhibited sugar accumulation in the aril. These results indicated an apoplasmic post-phloem sugar transport from the funicle to the aril. Although facilitated diffusion might help sucrose uptake from the cytosol to the vacuole in cultivars with high soluble invertase, membrane ATPases in the aril, especially tonoplast ATPase, are crucial for aril sugar accumulation. The expression of a putative aril vacuolar membrane sucrose transporter gene (*LcSUT4*) was highly correlated with the sugar accumulation in the aril of litchi. These data suggest that apoplasmic transport is critical for sugar accumulation in litchi aril and that *LcSUT4* is involved in this step.

Keywords: ATPase • Carboxyfluorescein imaging • Post-phloem transport • Sugar accumulation • Sugar transporters.

Abbreviations: CF, carboxyfluorescein; CFDA, carboxyfluorescein diacetate; CLSM, confocal laser scanning microscopy; CWAI, cell wall acid invertase; DAA, days after anthesis; EB, eosin B; FM, fresh material; HT, hexose transporter; P-ATPase; plasma membrane ATPase; PCMBS, *p*-chloromercuribenzene sulfonate; qRT-PCR, quantitative real-time PCR; RT–PCR, reverse transcription–PCR; SAI, soluble acid invertase; SE, sieve element; SE–CC, sieve element–companion cell; SPS, sucrose phosphate synthase; SS, sucrose synthase; SUT, sucrose transporter; TMT, tonoplast monosaccharide transporter; V-ATPase, vacuolar ATPase.

Introduction

It is now well accepted that phloem unloading and metabolism of imported sugars in sink cells play a key role in the partitioning of photo-assimilates (Fisher and Oparka 1996, Patrick 1997, Viola et al. 2001). Phloem unloading has been defined as assimilates moving from sieve element–companion cell (SE–CC) complexes to sites of sink cells. Therefore, phloem unloading includes SE unloading, transfer across the SE–CC complex boundary, and post-phloem transport, i.e. transport through a diverse range of sink parenchyma cells (Oparka 1990, Patrick 1997). Usually studies of phloem unloading have failed to distinguish between SE unloading and the subsequent post-phloem transport because of the microscopic size of the SE–CC complex and their poor accessibility within sink organs.

Evidence from several plant species suggests that a symplastic pathway of SE unloading predominates in many sink organs (Patrick 1997). However, there is also clear evidence suggesting an apoplasmic SE unloading pathway in some fruit species such as apple (*Malus domestica*) (Zhang et al. 2004) and walnut (*Juglans regia*) (Wu et al. 2004). In tomato (*Solanum lycopersicum*) fruit and grape (*Vitis vinifera*) berry, a symplasmic pathway operates at the early stages, but an apoplasmic pathway occurs at the late stages of fruit development (Ruan and Patrick 1995, Zhang et al. 2006). In jujube (*Zizyphus jujuba*) fruit, the predominance of an apoplasmic phloem unloading pathway was interrupted with a symplasmic pathway at the middle stage (Nie et al. 2010). These results suggested that the unloading route differs according not only to sink types but also to sink development.

Post-phloem transport of sucrose into terminal sink organs can take symplastic and/or apoplastic routes depending on the type of organ and developmental state (Patrick 1997). The symplastic route depends on plasmodesmata connections existing

Plant Cell Physiol. 56(2): 377–387 (2015) doi:10.1093/pcp/pcu173, Advance Access publication on 27 November 2014, available online at www.pcp.oxfordjournals.org

between sink cells, while the apoplastic route depends on carrier-mediated electrogenic transporters. The symplastic route seems to be the predominant pathway in most tissues investigated, whereas the apoplasmic step is largely associated with sinks which accumulate high concentrations of soluble sugars (Patrick 1997). Disruption of the symplasmic continuity within the stalks of juice vesicles and tracing of ^{14}C-labeled assimilates suggest an apoplasmic post-phloem transport in grapefruit (*Citrus paradisi*) (Koch and Avigne 1990). Post-phloem transport in apple fruit involves both apo- and symplasmic pathways occurring simultaneously, as indicated by the presence of plasma membrane-located putative monosaccharide transporter in parenchyma cells and numerous plasmodesmata connecting these cells (Zhang et al. 2004). Simultaneous symplasmic and apoplasmic unloading pathways in post-phloem transport have been reported during Chinese jujube fruit development (Nie et al. 2010).

Litchi (*Litchi chinensis* Sonn.) is one of the most important subtropical fruits. The edible part of litchi is the aril, which accumulates sugars amounting to 15–20% of the fresh mass. However, little is known about the unloading pathway in the developing litchi fruit. Unlike other fruit species, the flesh of litchi (aril) is an organ with no vascular tissue. The seed stalk or funicle, where the aril originates, serves as the connection between the vascular pedicel and the aril (**Fig. 1**). This special structure enables the distinction between SE unloading and post-phloem transport.

The involvement of apoplastic post-phloem transportation in assimilate import to fruit flesh makes it important to study the sugar transporters. Functional sucrose and hexose transporter genes have been cloned from various plant species. Expression and characterization of two sucrose transporters, SUC1 and SUC2, from *Arabidopsis thaliana* were described by Sauer and Stoltz (1994). *ShSUT1* was isolated from sugarcane, which displayed a K_m of approximately 200 mM for sucrose in *Saccharomyces cerevisiae* (Rae et al. 2005). In rice, five sucrose transporters (SUTs) were isolated and the expression pattern of each member was investigated (Aoki et al. 2003). Elevated transcript levels of tonoplast monosaccharide transporters (TMTs) were observed concomitant with accumulation of fructose in apple fruit (Li et al. 2012). In grape berries, the expression of two hexose transporter (HT) family genes, one TMT and one vacuolar glucose transporter (vGT) corresponds to massive accumulation of glucose and fructose in the vacuole (Afoufa-Bastien et al. 2010). However, no sugar transporter has been reported in litchi yet.

Sugar content and composition are one of the important determinants of the quality and flavor of fresh fruits. Sucrose, fructose and glucose are the principal sugars in litchi aril, and their accumulation varies among cultivars (Yang et al. 2013). Sucrose metabolism enzymes including invertase (EC 3.2.1.26), sucrose synthase (SS; EC 2.4.1.13) and sucrose phosphate synthase (SPS; EC 2.4.1.14) have been investigated in relation to sugar accumulation in citrus (Komatsu et al. 1999, Komatsu et al. 2002), peach (Vizzotto et al. 1996), tomato (Ngugen-Quoc and Foyer 2001) and banana (Choudhury et al. 2009). However, in the aril of litchi, the sugar concentration was found to have no link with sucrose metabolic enzymes (Yang et al. 2013). The mechanisms underlying sugar accumulation in litchi is an open question.

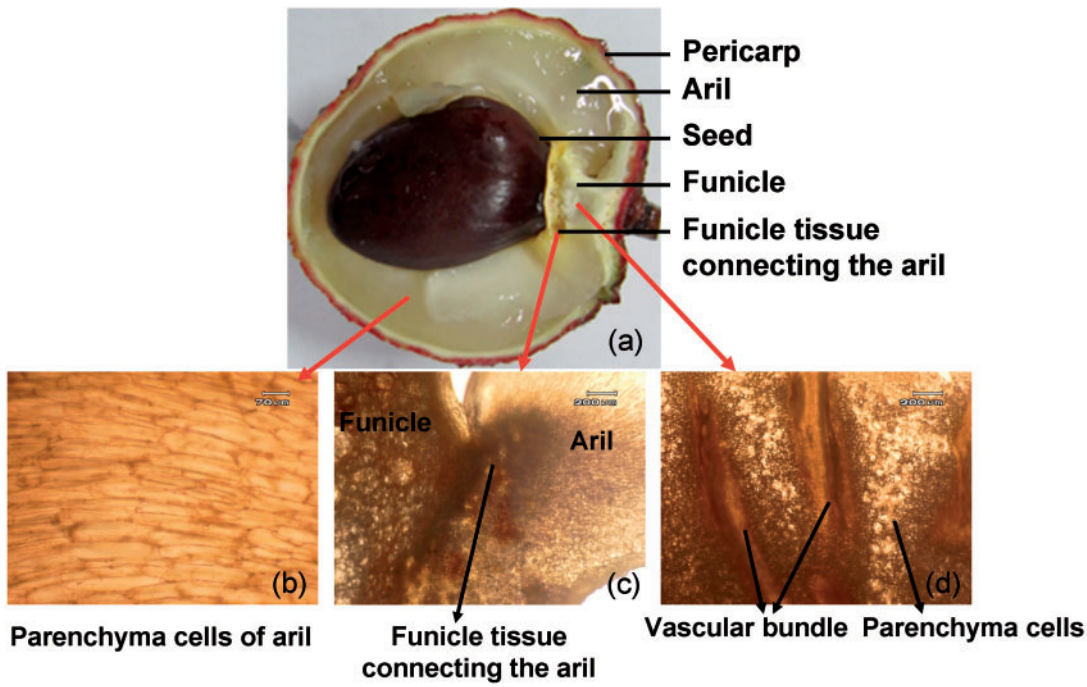

Fig. 1 Structure of litchi fruit. (a) Longitudinal section of a mature litchi fruit, showing various fruit structures. (b) A longitudinal section of the aril with no vascular bundle. (c) A longitudinal section of the funicle adjoining the aril with no vascular bundle. (d) A longitudinal section of the funicle consisting of the vascular bundles and spongy tissues.

An understanding of the transport and metabolic pathways associated with soluble sugar accumulation in litchi fruit may lead to novel selection criteria or molecular genetic strategies to improve litchi fruit soluble sugar levels. In the present study, four genotypes that differ significantly in soluble sugar content were studied in cultivars Nuomici (NMC), Feizixiao (FZX), Wuheli (WHL) and Heiye (HY), which had a total soluble sugar content of 193.2 ± 8.9, 187.6 ± 9.8, 164.5 ± 7.3 and 137.1 ± 16.3 mg g^{-1} fresh material (FM), respectively. The continuity of the symplasmic pathway between the funicle and aril was examined using the phloem-mobile tracer carboxyfluorescein (CF). The structures of the funicle and aril were observed using electron microscopy, enzyme activities of H^+-ATPase and gene expression of sugar transporters were analyzed, and the roles of ATPase and SUTs were examined using their corresponding inhibitors. The purposes of this study were to explore the phloem unloading pathway and the mechanism of aril sugar accumulation in litchi.

Results

Fruit structure and transportation of CF

A litchi fruit is a typical arilate fruit with its pericarp originating from the ovary wall and an aril as the edible part. Anatomical observations showed that the vascular bundles of litchi fruit end in the funicle (**Fig. 1**). No vascular bundle could be found in the aril and the connection area of the aril and funicle. Thus funicle is the sole corridor from the phloem to the aril.

Non-fluorescent carboxyfluorescein diacetate (CFDA) is degraded into CF when it is loaded into cells. CF is often used as a fluorescent marker of symplastic phloem unloading (Zhang et al. 2004), as its behavior is similar to the pattern of photoassimilate unloading determined by autoradiography (Viola et al. 2001). CFDA was supplied to the pedicel of litchi at three different stages of fruit development (**Fig. 2a**). At late stage (Stage III), an abscission layer appeared between the aril and the funicle and therefore the funicle could easily be separated from the seed and aril (**Fig. 2b**). Confocal laser scanning microscopy (CLSM) images of CF movement in the funicle and aril sampled 24 h after treatments are presented in **Fig. 2c–h**. CF was transported along the vascular bundle and diffused to the surrounding parenchyma cells in the funicle at all stages of fruit development. Distinct CF distribution was found in the connection area of the aril and funicle without apparent diffusion to the aril cells at the early (**Fig. 2f**) and middle (**Fig. 2g**) stage of fruit development. At the late stage of fruit development, CF was confined to the funicle with no distribution in the aril (**Fig. 2h**), which was probably due to the symplastic interruption in the connection area of the aril and funicle.

Plasmodesmatal frequencies

The frequencies of plasmodesmata in the cells of the funicle, the connection area of the aril and funicle and the ail in cultivar FZX are shown in **Fig. 3**. When expressed on a unit-of-shared-wall basis, funicle cells had particularly abundant plasmodesmata (**Fig. 3a**). Fewer plasmodesmata in the connection area of the aril and funicle and in the aril (**Fig. 3b, c**) were observed. The average number of plasmodesmata in the cells of the funicle was 1.79 ± 0.34 μm^{-1} of cell wall, which was about three and six times higher than in the connection area of the aril and funicle and in the aril, respectively (**Fig. 3d**).

Non-structural carbohydrate contents in the funicle

In the aril of litchi, sucrose, glucose and fructose are the predominant sugars (Paull et al. 1984, Yang et al. 2013). In the funicle, however, a relatively high level of oligomeric polysaccharide was observed in the ethanol extracts in addition to sucrose, glucose and fructose (**Fig. 4a**). The oligomeric polysaccharide was identified as a pentasaccharide consisting of two arabinose unites, two glucose units and one mannose unit using gas chromatography–mass spectrometry (GC-MS; data not shown).

The developmental changes in non-structural carbohydrates including soluble sugars and starch were analyzed in the funicle of the four litchi cultivars (**Fig. 4b**). Generally, the growth of the funicle was accompanied by increases in sucrose, glucose, fructose and total soluble sugars but a decrease in the pentasaccharide. Among the four cultivars, funicles in FZX and HY fruit contained much higher sucrose, glucose and fructose than those in NMC and WHL fruit, while the difference in the pentasaccharide was less apparent. These resulted in much higher soluble sugars in the funicles of FZX and HY fruit. The developmental patterns of starch varied among cultivars. Starch in the funicle increased from around 6 mg g^{-1} FM at 35 days after anthesis (DAA) to about 10 mg g^{-1} FM at 42 and 49 DAA in FZX and HY, respectively, but declined as fruit developed toward maturity. In NMC and WHL, however, starch contents in the funicles were much lower (around 3 mg g^{-1} FM) and remained relatively constant throughout fruit development.

Activities of plasma membrane and vacuolar ATPase in funicle and aril

H^+-ATPase behaves as a transducer, converting the chemical energy released from ATP hydrolysis into chemiosmotic energy, and therefore plays a central role in cross-membrane transport. In the present study, the activities of plasma membrane ATPase (P-ATPase) and vacuolar ATPase (V-ATPase) in the funicle and the aril throughout growth were detected (**Fig. 5a–d**). The activities of P-ATPase and V-ATPase in funicles remained relatively constant throughout growth. and no distinct pattern of activity difference was observed among the four tested cultivars (**Fig. 5a, b**). In the aril, however, the activities of P-ATPase tend to increase during the rapid aril sugar accumulation (**Fig. 5c**). Generally, cultivars HY and WHL displayed higher activities of P-ATPase than cultivars FZX and NMC before 56 DAA, while much higher P-ATPase activities were observed in the aril of NMC and WHL than in that of FZX and HY after 56 DAA. In both the funicle and aril, the activities of V-ATPase were much higher than those of P-ATPase (**Fig. 5**). Furthermore, the activities of V-ATPase in the sugar-rich aril were higher than in the

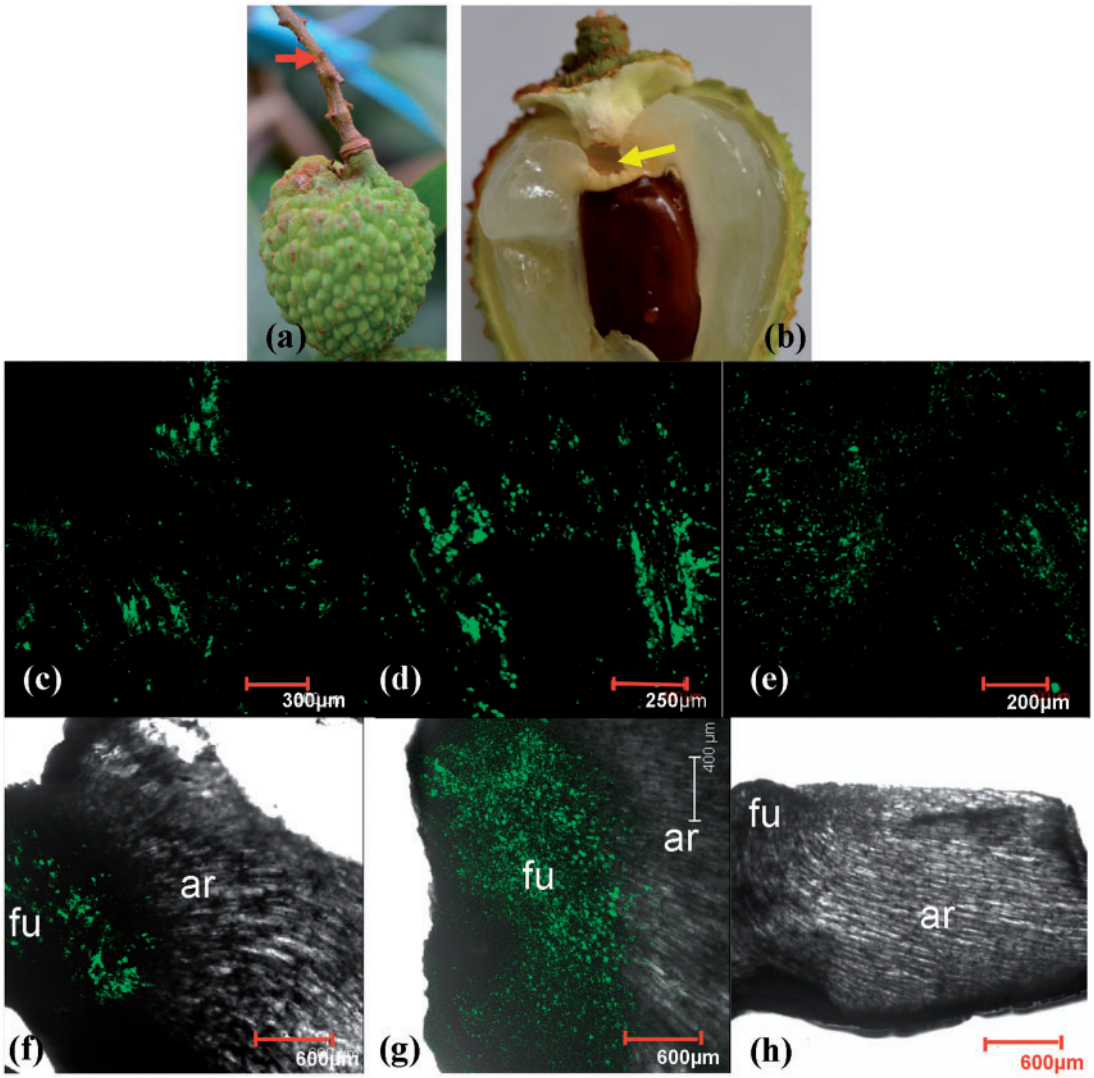

Fig. 2 Distribution of carboxyfluorescein (CF) introduced from the pedicel in the funicle (c–e) and aril (f–h). (a) An intact litchi fruit with fruit stalk from which CF was introduced (red arrow). (b) Separation of funicle from aril and seed in a maturing fruit (arrow). (c and f) Stage I. (d and g) Stage II. (e and h) Stage III. Ar, aril; fu, funicle.

funicle particulary in cultivars NMC and WHL. The developmental patterns of V-ATPase varied among cultivars. In the aril of FZX and HY, the V-ATPase activities remained low, and increased slightly as fruit developed toward full maturity. Much higher activities of V-ATPase were noticed in cultivars NMC and WHL compared with cultivars FZX and HY throughout aril growth. In cultivars NMC and WHL, the V-ATPase activities remained relatively constant during fruit growth. NMC aril had higher V-ATPase activities than WHL aril.

Expression of sugar transporter genes in the aril during fruit development

Five and seven ortholog genes of SUTs and HTs were identified in the genome of litchi. Among the identified *SUT* and *HT* genes, *LcSUT1*, *LcSUT4*, *LcHT2* and *LcHT5* displayed relatively high expression levels, whereas the remaining transporter genes were either expressed at extremely low levels or not expressed in the aril (**Supplementary Fig. S1**). *LcSUT1* shared high similarity with *HbSUT2B* and *AtSUC3* (**Supplementary Fig. S2**), which belongs to the SUC3/SUT2 group according to Aoki (2003). *LcSUT4* had the highest homology with *LjSUC4* and was clustered with *AtSUT4*, belonging to the SUC4 group (**Supplementary Fig. S2**). The transcript abundance of *LcSUT1* remained unchanged until an obvious rise from 56 DAA to full maturity. Higher expression levels of *LcSUT1* were observed in the arils of FZX and NMC before 56 DAA than in those of HY and WHL, while higher expression levels were noticed in WHL and FZX after 56 DAA (**Fig. 6a**). The expression levels of *LcSUT4* increased gradually toward maturity in FZX, HY and WHL, whereas in NMC its expression declined from 42 to 56 DAA and increased thereafter (**Fig. 6b**). Among the four cultivars tested, NMC displayed the highest expression levels of *LcSUT4*, followed by FZX and HY, while WHL showed the lowest transcript abundance.

The isolated *LcHT2* shared high similarity with *OlpGlT*, a hexose transporter isolated from *Olea europaea* (**Supplementary Fig. S3**). The transcript levels of *LcHT2*

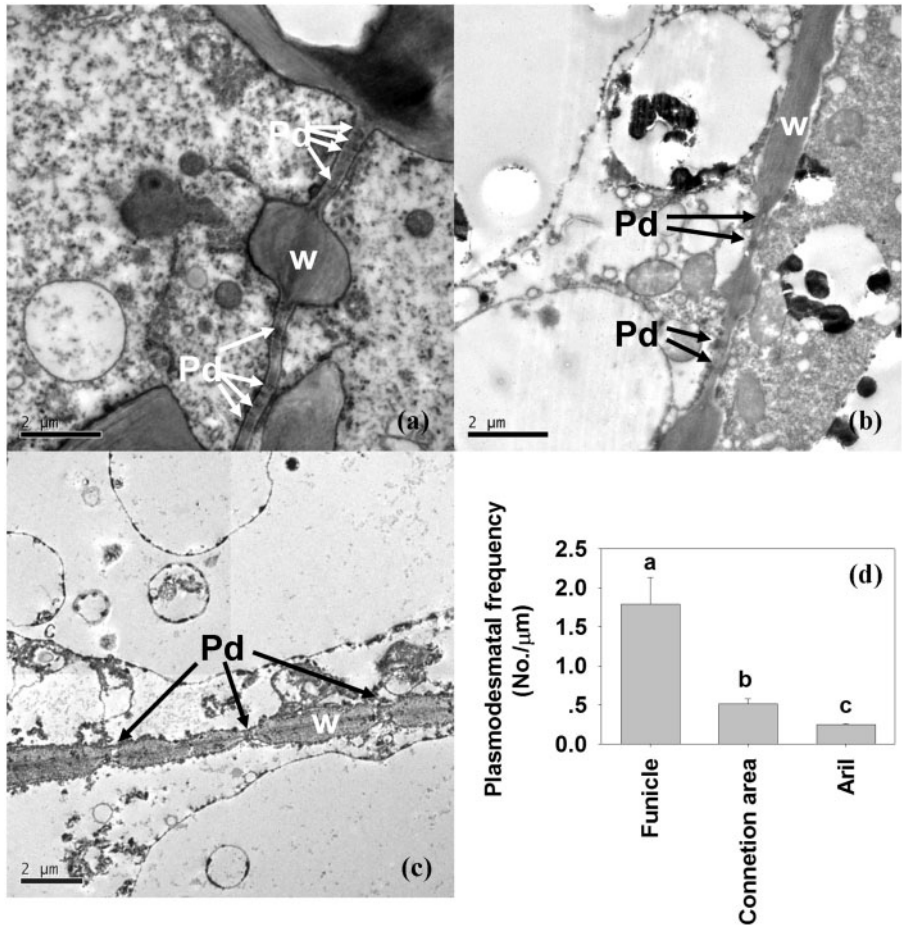

Fig. 3 The ultrastructure of the funcile (a), the funicle tissue adjoining the aril (b) and the aril (c) and the plasmodesmatal frequencies between parenchyma cells of these tissues (d) in cultivar FZX. The vertical bars represent the standard error of five replicates.

dropped throughout fruit growth in all the four cultivars tested (**Fig. 6c**). WHL displayed higher expression levels of *LcHT2* than the other three cultivars. The isolated *LcHT5* shared low similarity with other *HT* genes (**Supplementary Fig. S3**). The change in pattern varied among cultivars (**Fig. 6d**). The expression levels of *LcHT5* were high at the first and second sampling dates and then decreased later on in FZX. In the other cultivars, the expression levels remained low and relatively constant throughout fruit growth.

Effects of EB and PCMBS on aril sugar accumulation

To assess whether a sucrose transporter and ATPase are involved in aril sugar accumulation in litchi fruit, EB, an ATPase inhibitor, and PCMBS, a sucrose transporter inhibitor, were introduced into the fruit flesh by an infiltration technique used previously in our laboratory (Wang et al. 2007). In the presence and absence of EB and PCMBS, sugar uptake by the aril was calculated by determining the sugar contents at 0 and 7 d after infiltration. The effects of EB and PCMBS on the sugar accumulation in the aril of cultivars FZX and NMC are shown in **Fig. 7a–d**. In control arils of FZX, the weekly sugar increments were 3, 22, 35 and 61 mg g^{-1} FM, for sucrose, glucose, fructose and total sugars, respectively, and they were 22, 20, 24 and 66 mg g^{-1} FM in the control arils of NMC (**Fig. 7a, b**). These results were expected because the arils were actively accumulating sugars from 49 to 56 DAA. Significantly reduced increments of sucrose, glucose, fructose and therefore total sugars were observed in the presence of EB and PCMBS in both FZX and NMC. The aril of cultivar FZX when infiltrated with EB and PCMBS accumulated >90% less sucrose and about 25–45% less glucose, fructose and total sugars (**Fig. 7c**). The inhibitory effects of EB were more pronounced than those of PCMBS in the aril of NMC, as the aril treated with EB had about a 10% reduction in sucrose concentration and accumulated 30–65% less glucose, fructose and total sugars, while the aril treated with PCMBS accumulated about 40% less sucrose and 20% less fructose and total sugars as compared with control aril (**Fig. 7d**).

Discussion

Differential post-phloem transport pathways in diverse parenchyma cells of litchi

Phloem unloading into most tissues is currently thought to be symplastic, through plasmodesmata linking the cells in the sink

region (Minchin and Lacointe 2005). Therefore, the end of the symplastic flow is within the receiver cells. In litchi fruit, phloem transport ended in the funicle, and the spongy parenchyma funicle cells were the first cells to receive the photo-assimilates (**Fig. 1**). A symplastic connection existed between vascular tissue and funicle parenchyma cells, as reflected by the presence of CF dye (**Fig. 2**). In addition, abundant plasmodesmata were observed in funicle parenchyma cells (**Fig. 3**). These results provide direct evidence for symplasmic post-phloem transport in the funicle.

In the funicle of litchi, the osmotic pressure was kept low due to the conversion of soluble sugars into less osmotically active polymorphic forms (starch and pentasaccharide) (**Fig. 4a, b**). This strategy facilitated the symplastic flow of the solution from the phloem by increasing the difference in sugar concentration. Among the four cultivars tested, the funicles of FZX and HY displayed significantly higher activities of cell wall acid invertase (CWAI) and soluble acid invertase (SAI) as well as total sugars than those of NMC and WHL (Yang et al. 2014; **Fig. 4b**). Sucrose unloading and utilization depend on its cleavage into hexoses, which is catalyzed by SS and/or invertase (Ruan et al. 2010). It is currently accepted that the sucrose hydrolysis enzymes function in post-phloem transport by creating a sucrose gradient (Zhang et al. 2004, Nie et al. 2010). Symplastic transport depends on adequate plasmodesmata as well as a sucrose gradient (Patrick 1997). Significantly higher

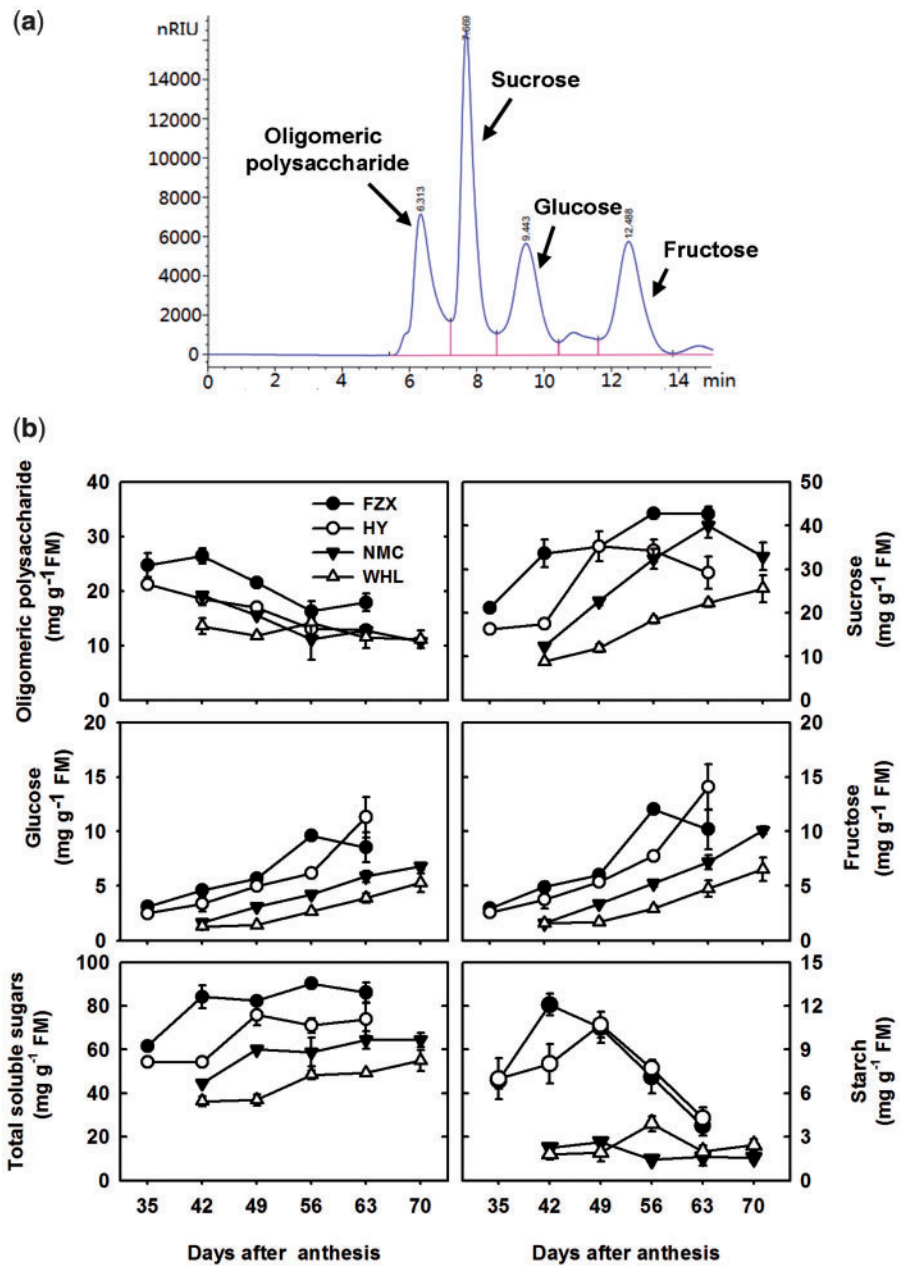

Fig. 4 HPLC elution profile of individual soluble sugars (a) and changes in the contents of soluble sugars and starch (b) in the funicle of four litchi cultivars during fruit development. The vertical bars represent the standard error of three replicates.

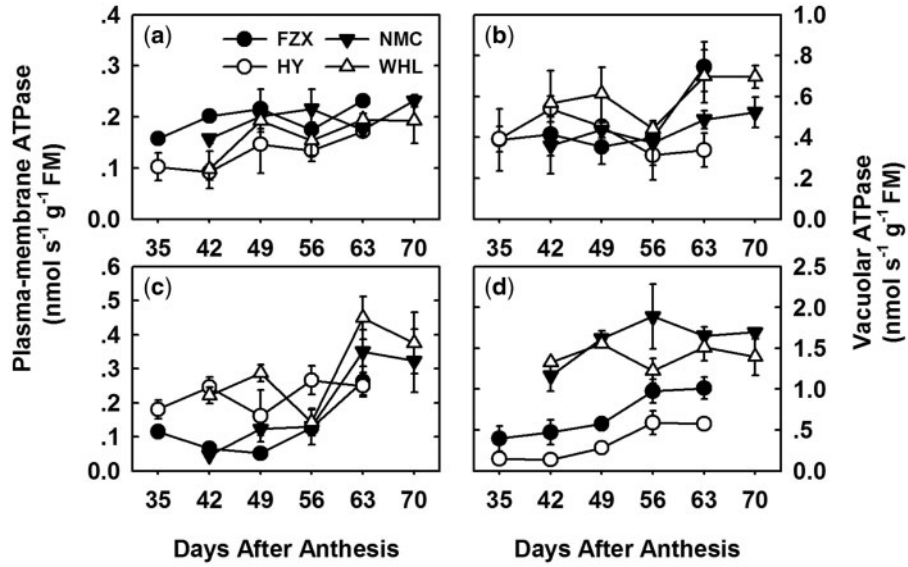

Fig. 5 Changes in the activities of plasma membrane and vaculoar ATPase in the funicle and aril during fruit development. (a) Plasma menbrane ATPase in the funicle. (b) Vacuolar ATPase in the funicle. (c) Plasma menbrane ATPase in the aril. (d) Vacuolar ATPase in the aril. The vertical bars represent the standard error of three replicates.

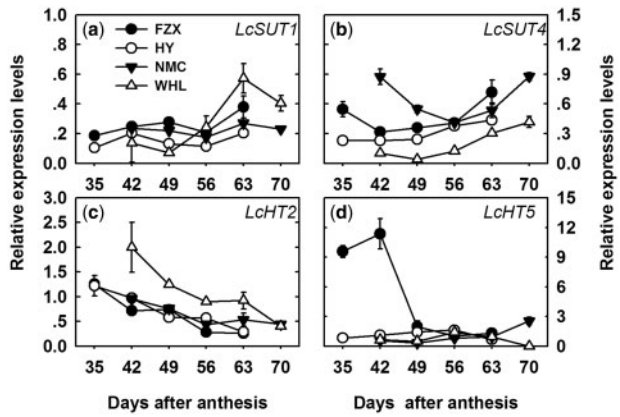

Fig. 6 Changes in the expression of *LcSUT1* (a), *LcSUT4* (b), *LcHT2* (c) and *LcHT5* (d) as determined by quantitative real-time PCR in the litchi aril of four cultivars during fruit development. The *Lcactin* gene was used to normalize gene expression under identical conditions. The vertical bars represent the standard error of three replicates.

starch and soluble sugar levels with higher activities of CWAI and SAI were observed in the funicle of FZX and HY compared with WHL and NMC. These provide additional support for a symplastic post-phloem transport process operating in the funicle of litchi.

Imaging of CF showed that the dye remained confined to the parenchyma cells of funicle tissue connecting the aril (**Fig. 2**), indicating that symplastic flow ends in the area of connection between the aril and the funicle. The aril of litchi fruit is apparently symplasmically separated from the funicle. An indirect approach to distinguish between apoplastic and symplastic transport is to analyze the effects of EB and/or PCMBS on sugar accumulation. PCMBS blocks carrier-mediated uptake of sugars from the apoplast (Ruan et al. 2001, Zhang et al. 2004). EB inhibited ATPase by abolishing the redox-induced proton extrusion (McDonald et al. 1996). Our study found that both EB and PCMBS inhibited sugar uptake into the aril (**Fig. 7**), suggesting that energy-driven transporters are involved in sugar accumulation of litchi aril. These data provide clear evidence for an apoplasmic post-phloem pathway from the funicle to the aril in litchi.

As a matter of fact, studies have suggested that the apoplasmic step is generally associated with sinks which accumulate high concentrations of soluble sugars (Patrick 1997, Zhang et al. 2004, Zhang et al. 2006). In the present study, >2-fold higher concentrations of sucrose, glucose and fructose were measured in the aril than in the funicle (**Fig. 4b**; Yang et al. 2013) and the existence of sucrose and hexose transporters in the aril of litchi provides additional support for apoplasmic post-phloem transport.

The role of membrane ATPase in the aril sugar accumulation of litchi

The quality of fresh fruit is largely determined by the content of soluble solids, with soluble sugars being the major component. The total amount of sugars accumulated in the aril of litchi varies among cultivars (Yang et al. 2013). Knowledge about the sugar accumulation mechanism in litchi fruit is, however, still fragmentary.

It is well accepted that sugars are transported into the sink cells by either simple diffusion along a steep concentration difference or a transporter-mediated and energy-coupled process. In litchi, sugar concentrations in aril are much higher than those in the funicle (**Fig. 4b**; Yang et al. 2013). Furthermore, previous studies have found no link between sucrose hydrolysis enzymes and the sugar accumulation in the aril of litchi (Yang et al. 2013). Thus, energy-driven transporters and energy metabolism rather than the sugar gradient created by sucrose hydrolysis might play crucial roles in determining sugar accumulation in the aril of litchi. Since the post-phloem

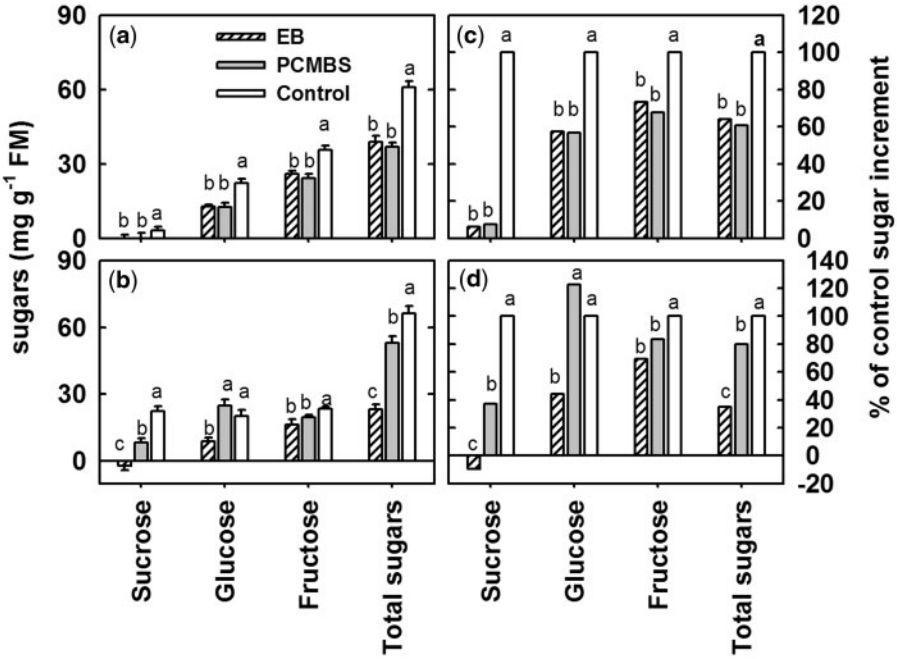

Fig. 7 Effects of EB and PCMBS on the sugar accumulation in the aril of cultivar FZX and NMC. (a) Sugar increment in the aril of FZX. (b) Sugar increment in the aril of NMC. (c) Percentage control sugar increments in the aril of FZX. (d) Percentage control sugar increments in the aril of NMC. The vertical bars represent the standard error of eight replicates.

movement of sugars into aril cells occurs through the apoplasmic pathway, key rate-limiting steps in sugar accumulation may reside at the plasmalemma and/or tonoplast.

In the apoplasmic pathway, sugars are transported into the sink cells, with protons moving in along the electrochemical gradient generated by a P-ATPase (Sondergaard et al. 2004). The vacuole is the largest plant organelle, and functions as a sink compartment for accumulation of sugars and other metabolites. The V-ATPase creates a proton motive force that is used to establish metabolite gradients across the vacuolar membrane (Krebs et al. 2010). In litchi, the activities of P-ATPase and V-ATPase increased generally in parallel with sugar accumulation in the aril (**Fig. 5c, d**).

In the present study, the arils of NMC and FZX accumulated 193.2 ± 8.9 and 187.6 ± 9.8 mg g^{-1} FM soluble sugars, respectively, which are significantly higher than the values in WHL (164.5 ± 7.3 mg g^{-1} FM) and HY (137.1 ± 16.3 mg g^{-1} FM). No obvious correlation was observed between aril sugar content and P-ATPase activity among different cultivars (**Fig. 5c**). A significant difference in the activities of V-ATPase was noticed among cultivars (**Fig. 5d**). FZX and HY displayed much lower activities of V-ATPase than cultivars NMC and WHL. Our previous study found that FZX and HY accumulated predominantly hexose due to higher activity of acid invertase, while NMC and WHL accumulated predominantly sucrose with low activities of acid invertase in the aril (Yang et al. 2013). Isolated vacuoles from sugarcane suspension cells take up sucrose at high rates independently of energization of the tonoplast but were inhibited by PCMBS (Preisser and Komor 1991, Preisser et al. 1992). These findings support the idea that sucrose accumulation in sugarcane vacuoles is primarily via a system of facilitated transport. In sweet lime, a species containing high levels of sucrose hydrolytic activity in the vacuole of juice cells, sucrose uptake into vacuoles occurs by facilitated diffusion (Echeverria et al. 1997). In the present study, FZX and HY with higher SAI activities and therefore high hexose/sucrose ratios had significantly lower activities of V-ATPase than NMC and WHL which had lower SAI activities and hexose/sucrose ratios. The hydrolytic action of acid invertase converting sucrose into hexoses within the vacuole might enhance facilitated diffusion and reduce the energy requirement for the uphill transportation of sucrose across the tonoplast; therefore, cultivars such as FZX and HY with lower a V-ATPase activity, which is compensated by a higher SAI activity, require less input of energy for sugar accumulation.

Due to the differences of SAI activity, the aril of different cultivars accumulated different types of sugars, giving rise to cultivar types with different sugar composition, a sucrose-dominant type and a hexose-dominant type. In cultivars with the same sugar composition type, those with higher aril sugar showed higher activities of V-ATPase (FZX vs. HY, NMC vs. WHL; **Fig. 5d**). EB, an ATPase inhibitor, significantly retarded the sugar accumulation in both cultivars, with this being more prominent in sucrose-dominant NMC than in hexose-dominant NMC (**Fig. 7a, d**). These results indicated that the sugar accumulation in the aril of litchi depended on the electrochemical gradient generated by V-ATPase and that the rate-limiting steps might reside in the tonoplast.

The role of sugar carriers in the aril sugar accumulation of litchi

As mentioned above, an active transport mechanism was required for the aril sugar accumulation of litchi. Sugar

transporters in the plasma and vacuolar membranes are responsible for moving sugars from the extracellular cell wall space into the cytosol and from the cytosol to the vacuole, respectively. Various sucrose transporters have now been found to be strongly expressed in grape berry (*VvSUC11*, *VvSUC12* and *VvSUC27*; Davies et al. 1999), citrus (*CitSUT1* and *CitSUT2*; Li et al. 2003) and tomato (*LeSUT1* and *LeSUT2*; Hackel et al. 2006). In the present study, five sucrose transporters have been cloned in litchi. Among them, *LcSUT1* and *LcSUT4* were expressed strongly in the aril (**Supplementary Fig. S1**). *LcSUT1* shared high similarity with the SUC3/SUT2 group, while *LcSUT4* shared high similarity with the SUC4/SUT4 group (**Supplementary Fig S2, S3**). Up-regulation of sucrose carrier proteins suggests that active transport of sucrose is enhanced during aril growth (**Fig. 6a, b**). During our experiments, we noted that stronger expression of *LcSUT4* coincided with higher sugar contents in the aril (**Fig. 6**). However, the expression of *LcSUT1* showed no connection with the sugar contents across the four cultivars.

Within a phylogenetic tree of plant sucrose transporters, the SUC4 branch (also known as the SUT4 branch) is well separated from other branches (Sauer 2007). When heterologously expressed in baker's yeast (*Saccharomyces cerevisiae*) or *Xenopus laevis* oocytes, *AtSUC4* from Arabidopsis, *StSUT4* from potato (*Solanum tuberosum*) and *LjSUT4* from *Lotus japonicus* appear to be associated with pH-dependent uptake of extracellular sucrose (Weise et al. 2000, Weschke et al. 2000, Reinders et al. 2008). Proteomic studies using purified vacuolar membranes suggested localization of *AtSUC4* and its barley (*Hordeum vulgare*) homolog *HvSUT2* to the tonoplast (Endler et al. 2006, Reinders et al. 2008). Further work is needed to determine the exact localization of *LcSUT4*. Overall, our data provide genetic proof that apoplasmic transport is critical for aril sugar accumulation in litchi aril and that *LcSUT4* is involved in sugar uptake by the cells in this tissue. The inhibitory effect of PCMBS on sugar accumulation provided further evidence for the crucial role of sugar transporter in aril sugar accumulation (**Fig. 7a–d**).

Although it remains unknown whether HTs are present on the plasma and/or tonoplast membrane, two HT genes, *LcHT2* and *LcHT5*, were expressed in the aril of litchi (**Fig. 6c, d**). In apple fruit, the transcript levels of *MdTMT1* and *MdTMT2* showed similar developmental trends to the fructose concentration, suggesting that both proteins may be involved in transporting fructose into the vacuole (Li et al. 2012). In contrast, the expression of *LcHT2* and *LcHT5* was not paralleled by the increase in hexose concentration in the aril of the four cultivars tested (**Fig. 6c, d**). Further work is needed to clarify their roles in sugar accumulation in litchi fruit.

In summary, the aril is symplastically separated from the funicle from which it grows. Therefore, sugar transport to the aril depends upon the apoplasmic pathway, and the uploading of sugars into the aril cells is an ATPase-dependent active process that involves actions of the plasma membrane proton pump and the putative transporter *LcSUT4*.

Materials and Methods

Plant materials

Fruit from three trees each of FZX, HY, NMC and WHL were sampled to determine the developmental patterns of total sugar contents, sugar composition, activities of enzymes and expression of sucrose and hexose transporters in the funicle and aril. Fruits were sampled at intervals of 7 d from 35 DAA (FZX and HY) or 42 DAA (NMC and WHL), i.e. 10 d after aril emergence, until full maturity. The trees grown at the experimental orchard of South China Agricultural University, Guangzhou, China received standard horticultural practices and disease and insect control. Immediately after harvest, the funicles and arils were separated, frozen immediately in liquid nitrogen and stored at −80°C until used.

Carboxyfluorescein diacetate (CFDA) labeling

The CFDA labeling was done as described previously (Zhang et al. 2004). Eight fruit each from FZX and NMC were infiltrated on-tree with 0.5 ml of 1 mg ml^{-1} CFDA solution at 42, 56 and 70 DAA. The CFDA solution was introduced into the fruit pedicel by a piece of cotton thread with one end immersed in an Eppendorf tube filled with CFDA, the other end forced through the pedicel with a needle and the whole piece of thread wetted with the CFDA solution. Fruit were allowed to take up CFDA solution for 24 h before they were harvested and dissected.

Tissue sectioning and microscopy

Before examination by CLSM, the pedicel, funicle and aril from the CFDA-treated fruit were carefully cut into transversal or longitudinal sections and immediately immersed in 80% (v/v) glycerol. A Bio-Rad MRC 1024 confocal laser scanning microscope was used to image CFDA distribution (with excitation at 488 nm and emission at 515 nm).

Aril and pedicel cut into longitudinal sections were observed under an OLYMPUS DP70 light microscope.

Plasmodesmal frequency

Plasmodesmal frequency was determined according to Zhang et al. (2004). Five group series of longitudinal ultrathin sections were prepared from the Spurr-infiltrated samples. From each group, three pieces of ultrathin sections were picked at random and put on the copper grids of 100× meshes. Five areas from each ultrathin section were observed under a TECNAI 12 transmission electron microscope. Plasmodesmata were counted at all cell interfaces. Plasmodesmal frequency is given as the number of plasmodesmata per micron of specific cell/cell interface length on longitudinal section.

The contents of soluble sugars and starch

Soluble sugars were measured by HPLC. Determinations were carried out as described by Yang et al. (2013). For arils, 1 g of tissue was homogenized and extracted with 10 ml of water, and then centrifuged for 10 min at 16,000×*g*. For the funicle, tissue (0.3 g) was homogenized and extracted three times with 85% (v/v) ethanol (3 ml each time). The pooled supernatant was rotary evaporated to dryness and re-suspended in 2 ml of distilled water. Sugars were detected by an Agilent 1200 HPLC system (Agilent Technologies) equipped with a refractive index detector and a transgenomic CARB Sep Coregel 87C column (CHO-99-5860). Sugars were identified by comparing their retention time with those of authentic standards, and concentrations of individual sugars were quantified based on peak area and calibration curves derived from authentic standards. An unknown oligomeric polysaccharide was noticed in the extracts of the funicle. The oligomeric polysaccharide fraction was collected using a fraction collector, dried at low pressure by a rotary evaporator, and hydrolyzed by trifluoroacetic acid. The released monosaccharides were detected by GC-MS after derivatization according to Wang et al. (2010).

The residual pellet after soluble sugar extraction was boiled in 2 ml of 0.2 M KOH for 30 min, adjusting the pH to 4.5 with 1 ml of 1 M acetic acid, and then it was digested with 50 U of amyloglucosidase (EC 3.2.1.3) at 55°C for 30 min. Starch was determined as glucose equivalents according to Wang et al. (2010).

The treatment of EB and PCMBS

The EB and PCMBS were introduced into the fruit in the same way as CFDA, as described above. The fruit were treated on-tree with EB or PCMBS solution at 49 DAA for cultivars NMC and FZX. On-tree fruit were treated with approximately 0.5 ml of 0.1 mg ml^{-1} EB or 5 mg ml^{-1} PCMBS aqueous solution (freshly prepared). Fruit treated with water were taken as the control. Fruit were harvested on the day of treatment and 7 d after treatment. The soluble sugars in the aril were analyzed by HPLC and the sugar increments within the 7 d after treatment were calculated.

Assays of plasma and vacuolar membrane H^+-ATPase

Membrane vesicles were prepared according to the methods of Faraday and Spanswick (1992). All steps were carried out at 4°C. Briefly, the collected aril samples were ground in ice-cold homogenization buffer (pH 8.0) (1 : 4 w/v) containing 100 mM Tris–HCl, 250 mM sucrose, 10% (v/v) glycerol, 2 mM EDTA, 1 mM $MgCl_2$, 5 mM dithiothreitol (DTT), 1 mM phenylmethylsulfonyl fluoride (PMSF), 1% (w/v) polyvinylpyrrolidone (PVPP), 5 mM ascorbic acid and 1 μM leupeptin. The homogenate was filtered through four layers of cheesecloth and centrifuged at 10,000×*g* for 30 min. The supernatant was then centrifuged at 100,000×*g* for 60 min. The microsomal pellet was suspended in phase buffer (250 mM sucrose, 4 mM KCl, 1 mM DTT, 0.5 mM PMSF, 5 mM potassium phosphate buffer, pH 7.8). The microsome was added to an 8 g two-phase system consisting of 6.7% (w/w) Dextran T500 (Pharmacia, Sweden), 6.4% (w/w) polyethylene glycol 3350 (PEG3350; Sigma), 1 mM sucrose and 22.7 mM KCl. After centrifugation, the upper phase was collected and dissolved in the microsome suspension solution and centrifuged at 100,000×*g* for 60 min. The plasma membrane pellet was collected and suspended in 1 ml of 25 mM HEPES-NaOH buffer (pH 7.5) containing 250 mM sucrose, 1 mM DTT and 0.5 mM PMSF.

ATPase hydrolysis assays were performed according to Briskin and Reynolds-Niesman (1991). The plasma membrane H^+-ATPase activity was assayed in a mixture containing 30 mM TRIS-MES (pH 6.13), 3 mM $MgSO_4$, 50 mM KCl, 1 mM $NaMoO_2$, 0.01% (v/v) Triton X-100, 50 mM KNO_3, 1 mM NaN_3, 0.15 mM NADH, 0.42 mM phosphoenolpyruvic acid, 3 mM ATP, 2 U of lactate dehydrogenase, 5 U of pyruvate kinase and 0.1 ml of enzyme extract. The reaction mixture for tonoplast H^+-ATPase activity was generally the same as that for plasma membrane H^+-ATPase with 50 mM KNO_3 replaced by 1 mM $Na_3V_3O_4$ and the pH value adjusted to 6.50. The enzyme activities were measured as the rate of change in absorbance at 340 nm using a spectrophotometer (Shimadzu UV-1800).

Quantitative real-time PCR analysis

Total RNA was extracted from funicle using the Quick RNA isolation kit (HUAYUEYANG). For real-time quantitative reverse transcription–PCR (RT–PCR), DNA-free RNA was converted into first-strand cDNA using the MLV-Reserve Transcriptase kit (Invitrogen). The total RNA from the aril was isolated using a modified hot borate method previously described by Wan and Wilkins (1994). ReverTra qPCR RT Master Mix gDNA Remover (TOYOBO) was used to purify and convert the total RNA.

Gene-specific primers (**Supplementary Table S1**) were designed using Primer 5.0 software. Primer specificity was determined by RT–PCR and melt curve analysis. The transcript levels were analyzed using quantitative real-time PCR (qRT-PCR) with THUNDERBIRD qPCR Mix (TOYOBO) and Lightcycler 480 Real-Time PCR Systems (Roche), which were used according to the manufacturers' protocol. Each reaction mixture (final volume, 10 μl) contained 4.5 μl of 2× SYBR® qPCR Mix (TOYOBO), 0.5 μl of the forward and reverse primers (0.25 μM), 1 μl of the cDNA template (corresponding to 50 ng of total RNA) and 4 μl of RNase-free water. PCR amplifications included the following conditions: 95°C for 30 s, followed by 40 cycles at 95°C for 5 s, 55°C for 30 s and 72°C for 30 s. All qRT-PCRs were normalized using the Ct value corresponding to *LcActin* (GenBank accession No. HQ588865.1). The relative expression levels of those genes were calculated using the $2^{-\Delta\Delta CT}$ method (Livak and Schmittgen 2001). Reported values represent the average of three biological replicates.

Statistical analysis

Statistical analyses were performed using the statistical package DPS v3.0. Duncan's multiple range test was used to determine the significance of plasmodesmal frequency and sugar increments at $P < 0.05$.

Supplementary data

Supplementary data are available at PCP online.

Funding

This study was supported by the China Litchi and Longan Industry Technology Research System [project No. CARS-33-11]; the National Natural Science Fund of China [project No. 31471838]. The funders had no role in study design, data collection and analysis, decision to publish or preparation of the manuscript.

Acknowledgments

We thank Guibing Hu for providing information on the plant materials, and Jietang Zhao for his technical assistance.

Disclosures

The authors have no conflicts of interest to declare.

References

Afoufa-Bastien, D., Medici, A., Jeauffre, J., Coutos-Thevenot, P., Lemoine, R., Atanassova, R. et al. (2010) The *Vitis vinifera* sugar transporter gene family: phylogenetic overview and macroarray expression profiling. *BMC Plant Biol.* 10: 245.

Aoki, N., Hirose, T., Scofield, G.N., Whitfeld, P.R. and Furbank, R.T. (2003) The sucrose transporter gene family in rice. *Plant Cell Physiol.* 44: 223–232.

Briskin, B.P. and Reynolds-Niesman, I. (1991) Determination of H^+/ATP stoichiometry for the plasma membrane H^+-ATPase from red beet (*Beta vulgaris* L.) storage tissue. *Plant Physiol.* 95: 242–250.

Choudhury, S.R., Roy, S. and Sengupta, D.N. (2009) A comparative study of cultivar differences in sucrose phosphate synthase gene expression and sucrose formation during banana fruit ripening. *Postharvest Biol. Technol.* 54: 15–24.

Davies, C., Wolf, T. and Robinson, S.P. (1999) Three putative sucrose transporters are differentially expressed in grapevine tissues. *Plant Sci.* 147: 93–100.

Echeverria, E., Gonzalez, P.C. and Brune, A. (1997) Characterization of proton and sugar transport at the tonoplast of sweet lime (*Citrus limmetioides*) juice cells. *Physiol. Plant.* 101: 291–300.

Endler, A., Meyer, S., Schelbert, S., Schneider, T., Weschke, W., Peters, S.W. et al. (2006) Identification of a vacuolar sucrose transporter in barley and Arabidopsis mesophyll cells by a tonoplast proteomic approach. *Plant Physiol.* 141: 196–207.

Faraday, C.D. and Spanswick, R.M. (1992) Maize root plasma membranes isolated by aqueous polymer two-phase partitioning: assessment of residual tonoplast ATPase and pyrophosphatase activities. *J. Exp. Bot.* 43: 1583–1590.

Fisher, D.B. and Oparka, K.J. (1996) Post-phloem transport: principles and problems. *J. Exp. Bot.* 47: 1141–1154.

Hackel, A., Schauer, N., Carrari, F., Fernie, A.R., Grimm, B. and Kühn, C. (2006) Sucrose transporter *LeSUT1* and *LeSUT2* inhibition affects tomato fruit development in different ways. *Plant J.* 45: 180–192.

Koch, K.E. and Avigne, W.T. (1990) Postphloem, nonvascular transfer in citrus: kinetics, metabolism, and sugar gradients. *Plant Physiol.* 93: 1405–1416.

Komatsu, A., Moriguchi, T., Koyama, K., Omura, M. and Akihama, T. (2002) Analysis of sucrose synthase genes in citrus suggests different roles and phylogenetic relationships. *J. Exp. Bot.* 53: 61–71.

Komatsu, A., Takanokura, Y., Moriguchi, T., Omura, M. and Akihama, T. (1999) Differential expression of three sucrose-phosphate synthase isoforms during sucrose accumulation in citrus fruits (*Citrus unshiu* Marc.). *Plant Sci.* 140: 169–78.

Krebs, M., Beyhl, D., Gorlich, E., Al-Rasheid, K.A., Marten, I., Stierhof, Y.D. et al. (2010) Arabidopsis V-ATPase activity at the tonoplast is required for efficient nutrient storage but not for sodium accumulation. *Proc. Natl Acad. Sci. USA* 107: 3251–3256.

Li, C.Y., Shi, J.X., Weiss, D. and Goldschmidt, E.E. (2003) Sugar regulate sucrose transporter gene expression in citrus. *Biochem. Biophys. Res. Commun.* 306: 402–407.

Li, M., Feng, F. and Cheng, L. (2012) Expression patterns of genes involved in sugar metabolism and accumulation during apple fruit development. *PLoS One* 7: e33055.

Livak, K.J. and Schmittgen, T.D. (2001) Analysis of relative gene expression data using real-time quantitative PCR and the $2^{-\Delta\Delta CT}$ method. *Methods* 25: 402–408.

McDonald, R., Fieuw, S. and Patrick, J.W. (1996) Sugar uptake by the dermal transfer cells of developing cotyledons of *Vicia faba* L.: mechanism of energy coupling. *Planta* 198: 502–509.

Minchin, P.E.H. and Lacointe, A. (2005) New understanding on phloem physiology and possible consequences for modeling long-distance carbon transport. *New Phytol.* 166: 771–779.

Ngugen-Quoc, B. and Foyer, C.H. (2001) A role for 'futile cycles' involving invertase and sucrose synthase in sucrose metabolism of tomato fruit. *J. Exp. Bot.* 52: 881–889.

Nie, P.X., Wang, X.Y., Hu, L.P., Zhang, H.Y., Zhang, J.X., Zhang, Z.X. et al. (2010) The predominance of the apoplasmic phloem-unloading pathway is interrupted by a symplasmic pathway during Chinese jujube fruit development. *Plant Cell Physiol.* 51: 1007–1018.

Oparka, K.J. (1990) What is phloem unloading?. *Plant Physiol* 94: 393–396.

Patrick, J.W. (1997) Phloem unloading: sieve element un-loading and post-sieve element transport. *Annu. Rev. Plant Physiol.* 48: 191–222.

Paull, R.E., Chen, N.J., Deputy, J., Huang, H.B., Cheng, G.W. and Gao, FF. (1984) Litchi growth and compositional changes during fruit development. *J. Am. Soc. Hortic. Sci.* 109: 817–821.

Preisser, J. and Komor, E. (1991) Sucrose uptake in vacuoles of sugarcane suspension cells. *Planta* 186: 109–114.

Preisser, J., Sprugel, H. and Komor, E. (1992) Solute distribution between vacuole and cytosol of sugarcane suspension cells, sucrose is not accumulated in the vacuole. *Planta* 186: 203–211.

Rae, A.L., Perroux, J.M. and Grof, C.P.L. (2005) Sucrose partitioning between vascular bundles and storage parenchyma in the sugarcane stem: a potential role for the *ShSUT1* sucrose transporter. *Planta* 220: 817–825.

Reinders, A., Sivitz, A.B., Starker, C.G., Gantt, J.S. and Ward, J.M. (2008) Functional analysis of *LjSUT4*, a vacuolar sucrose transporter from *Lotus japonicus*. *Plant Mol. Biol.* 68: 289–299.

Ruan, Y.L., Jin, Y., Yang, Y.J., Li, G.J. and Boyer, J.S. (2010) Sugar input, metabolism, and signaling mediated by invertase: roles in development, yield potential, and response to drought and heat. *Mol. Plant* 3: 942–955.

Ruan, Y.L., Llewellyn, D.J. and Furbank, R.T. (2001) The control of single-celled cotton fiber elongation by developmentally reversible gating of plasmodesmata and coordinated expression of sucrose and K^+ transporters and expansin. *Plant Cell* 13: 47–60.

Ruan, Y.L. and Patrick, J.W. (1995) The cellular pathway of postphloem sugar transport in developing tomato fruit. *Planta* 196: 434–444.

Sauer, N. and Stoltz, J. (1994) SUC1 and SUC2, two sucrose transporters from Arabidopsis thaliana; expression and characterisation in baker's yeast and identification of the histidine-tagged protein. *Plant J.* 6: 67–77.

Sauer, N. (2007) Molecular physiology of higher plant sucrose transporters. *FEBS Lett.* 581: 2309–2317.

Sondergaard, T.E., Schulz, A. and Palmgren, M.G. (2004) Energization of transport processes in plants. Roles of the plasma membrane H+-ATPase. *Plant Physiol.* 136: 2476–2482.

Viola, R., Roberts, A.G., Haupt, S., Gazzani, S., Hancock, R.D., Marmiroli, N. et al. (2001) Tuberization in potato involves a switch from apoplastic to symplastic phloem unloading. *Plant Cell* 13: 385–398.

Vizzotto, G., Pinton, R., Varanini, Z. and Costa, G. (1996) Sucrose accumulation in developing peach fruit. *Physiol. Plant.* 96: 225–30.

Wan, C.Y. and Wilkins, T.A. (1994) A modified hot borate method significantly enhances the yield of high-quality RNA from cotton (*Gossypium hirsutum* L.). *Anal. Biochem.* 223: 7–12.

Wang, H., Huang, H. and Huang, X. (2007) Differential effects of abscisic acid and ethylene on the fruit maturation of *Litchi chinensis* Sonn. *Plant Growth Regul.* 52: 189–198.

Wang, H.C., Ma, F.F. and Cheng, L.L. (2010) Metabolism of organic acids, nitrogen and amino acids in chlorotic leaves of 'Honeycrisp' apple (*Malus domestica* Borkh) with excessive accumulation of carbohydrates. *Planta* 232: 511–522.

Weise, A., Barker, L., Kühn, C., Lalonde, S., Buschmann, H., Frommer, W.B. et al. (2000) A new subfamily of sucrose transporters, SUT4, with low affinity/high capacity localised in enucleate sieve elements of plants. *Plant Cell* 12: 1345–1355.

Weschke, W., Panitz, R., Sauer, N., Wang, Q., Neubohn, B., Weber, H. et al. (2000) Sucrose transport into barley seeds, molecular characterisation of two transporters and implications for seed development and starch accumulation. *Plant J.* 21: 459–469.

Wu, G.L., Zhang, X.Y., Zhang, L.Y., Pan, Q.H., Shen, Y.Y. and Zhang, D.P. (2004) Phloem unloading in developing walnut fruit is symplasmic in the seed pericarp and apoplasmic in the fleshy pericarp. *Plant Cell Physiol.* 45: 1461–1470.

Yang, Z.Y., Wang, T.D., Wang, H.C., Huang, X.M., Qin, Y.H. and Hu, G.B. (2013) Patterns of enzyme activities and gene expressions in sucrose metabolism in relation to sugar accumulation and composition in the aril of *Litchi chinensis* Sonn. *J. Plant Physiol.* 170: 731–740.

Yang, Z.Y., Zhang, J.Q., Wang, T.D., Huang, X.M., Hu, G.B. and Wang, H.C. (2014) Does acid invertase regulate the seed development of *Litchi chinensis*? *Acta Hort. 1029* 301–307.

Zhang, L., Peng, Y.B., Pelleschi-Travier, S., Fan, Y., Lu, Y.F., Lu, Y.M. et al. (2004) Evidence for apoplasmic phloem unloading in developing apple fruit. *Plant Physiol.* 135: 574–586.

Zhang, X.Y., Wang, X.L., Wang, X.F., Xia, G.H., Pan, Q.H., Fan, R.C. et al. (2006) A shift of phloem unloading from symplasmic to apoplasmic pathway is involved in developmental onset of ripening in grape berry. *Plant Physiol.* 142: 220–232.